Streamlined Deamidation Assessment During Thermal Stress

With thanks to Curtis W. Meuse[1,2]
[1]Institute for Bioscience and Biotechnology Research, University of Maryland and [2]Biomolecular Measurement Division, National Institute of Standards and Technology, Rockville, MD, USA

Summary

- This Application Note illustrates the use of the ProteinMentor platform for a comparative assessment of a concentration series of a monoclonal antibody in solution.
- The unique combination of microscopy and spectroscopy, along with the ability to apply a thermal stress across an array of samples, provides for comparative deamidation analysis in a single experiment.
- Spectral analysis of the data provides detailed insight into the sites and extent of deamidation, along with insight into the impact of deamidation on protein stability.

Introduction

Recent years have seen an unprecedented growth in the development of biological molecules and biological products as therapeutic treatments for a wide variety of diseases. The challenges of formulating these products to optimize stability, preserve therapeutic efficacy and minimize immunogenicity are well-known to be far more complicated than traditional pharmaceutical products. One class of biological therapies that have been heavily focused on are therapeutic proteins, including monoclonal antibodies (mAb). According to the Antibody Society[1,2] there are approximately 100 approved antibody therapeutics in the EU and US, with an additional 18 in regulatory review.

Analytical methodologies to assess critical quality attributes (CQAs) of therapeutic proteins are varied, time-consuming and can involve complicated sample preparation and analysis.

Multiple analytical tools are routinely deployed for each CQA assessment, and the results provide limited understanding of how, and to what extent, each CQA impacts safety and efficacy. This fragmented approach contributes to the high cost, long timelines and increased risk of safety and efficacy of the therapeutic proteins.

Understanding deamidation at the molecular level is critical for the development and commercialization of therapeutic proteins. Comprehensive characterization and efficient monitoring of deamidation events and their potential impact on protein stability, self-

association and aggregation can effectively reduce the risk of immunogenicity. When applied within developability assessment, identification of deamidation risk can be used for sequence modification to improve biotherapeutic stability profiles. The approach can also be implemented for pre-clinical candidate selection during developability assessment.

In this application note, we describe the use of the ProteinMentor platform for the characterization and monitoring of a dilution series of the NISTmAb Primary Sample (PS 8670). The NISTmAb Reference Material (RM) 8671 is intended as an industry standard for pre-competitive harmonization and designing characterization technologies for identity, quality, and stability testing[3]. PS 8670 is the in-house primary sample, which can be used for lot-to-lot stability evaluation. This reference sample is very useful for assessing or confirming capabilities of a new technology. In our collaboration with NIST, we have used NISTmAb samples for assessing deamidation analysis using the ProteinMentor platform.

ProteinMentor is a unique combination of Quantum Cascade Laser (QCL) microscopy and spectroscopy which allows for the direct visualization of aggregates and the spectroscopic evaluation of molecular events that lead to structural changes, self-association and ultimately aggregation. We demonstrate the applicability of the platform for the assessment of deamidation. A detailed description of the full study has been published in the Encyclopedia of Analytical Chemistry (Pastrana & Meuse, 2022) see reference 3 for full details.

Methods

Samples

No sample preparative steps are needed to evaluate deamidation and stability. The sample is simply diluted to generate a dilution series. NISTmAb Primary Sample (PS 8670) was subject to a dilution using 25 mM L-histidine at pH 6.0. The resulting concentrations were 100, 70, 40, 10, 5 and 2.5 μg/μL. One μL of each sample was applied to the ProteinMentor slide cell array (SCA). The mAb samples are intact (full-length) and evaluated as such in their formulation for comparative assessment.

Instrumentation

The SCA was then placed in a heated accessory with (+/- 0.5 °C) thermal control. Hyperspectral (HS) images were acquired within the temperature range of 28 – 60 °C with 8 °C intervals and 4 min equilibration periods using ProteinMentor, a QCL IR transmission microscope. The HS images are composed of 223,000 QCLM spectra collected at 4 cm^{-1} spectral resolution within the spectral region of 1775 – 1500 cm^{-1}. For full experimental details see reference 1.

Data Processing

The HS images were analyzed using DataPDS™ software. Correlational analysis was performed using both two-dimensional infrared correlational spectroscopy (2D-COS) and two-dimensional co-distribution spectroscopy (2D-CDS) in the Correlation Dynamics™ software. QCLM spectral baseline correction, difference spectra overlays, 2D-CDS, and 2D-COS plots were generated using Correlation Dynamics™ software. For a comparative analysis we chose a temperature range below the onset of thermal transition to establish differences in stability that would not involve thermal unfolding to the point of denaturation.

Results and Discussion

Hyperspectral Images – Visual Inspection for Aggregation

ProteinMentor provides a visual indicator of aggregates greater than 4.3 µm in size, the spatial resolution of the system. For the study here, no visible aggregates were apparent, with clear, and featureless, homogenous solutions shown by the hyperspectral (HS) images (see reference 3 for HS images of NIST mAb at the high and low concentrations of 100 and 2.5 µg/µL).

Even in the absence of visual aggregation, however, aggregates smaller than 4.3 µm may be present. Evaluation of the spectral data from ProteinMentor is able to determine if any aggregation was induced by the deamidation event during the thermal stress imparted on the proteins. The spectral evaluation can also detect changes in protein structure, such as deamidation, that may lead to the onset of aggregation or other issues that impact therapeutic efficacy or immunogenicity.

Spectral Analysis and 2-Dimensional Correlation Spectroscopy

Each HS image is comprised of 223,000 QCL IRM spectra and takes about 40 seconds to acquire. Figure 1 displays a schematic with all the information that is obtained from a single microliter sample.

Evaluation of the spectral data focuses on the assignment and inspection of well-known peaks within IR spectra of protein samples[3]. The spectral overlays for 6 different concentrations of the NIST mAb ranging from 100 µg/µL down to 2.5 µg/µL are shown in Figure 2.

The Amide II band, between 1600 cm^{-1} and 1500 cm^{-1}, is where side chain amino acid modes are located. Visual inspection of this region as the concentration decreases from Figure 2A to Figure 2F shows the dilution effect with the decreasing absorbance of this band. The Amide I band (between 1700 cm^{-1} and 1600 cm^{-1}, has the overlapping water vibration, and therefore does not serve well for visual interpretation of the decreasing concentration.

The design of the ProteinMentor platform, with the QCL microscope and heated Slide Cell Array (SCA), provides an enhanced S/N with accurate thermal control and allows for the

difference spectra to be generated (Figure 1, step 3). The difference spectra are generated by simply subtracting the first spectrum from all subsequent spectra. This allows for the subtraction of the H_2O contribution and also removes any spectral contributions that did not change over the course of the thermal stress evaluation.

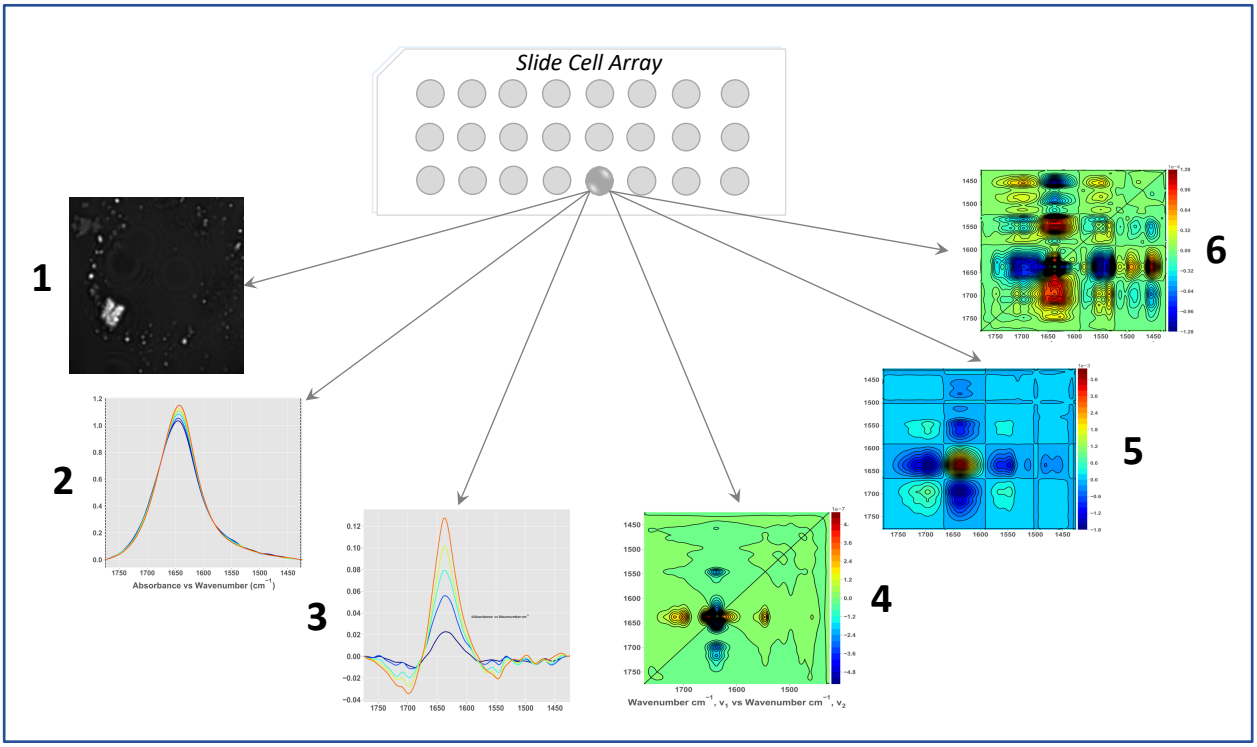

Figure 1: Schematic showing how ProteinMentor provides a wealth of information from a single 40 second analysis in a 1 µL sample. A schematic of the slide cell array with 21 samples and appropriate controls is shown at the top of the figure. For every NISTmAb sample concentration in the slide cell array, a series of HS images were acquired at every set temperature.

(1) Hyperspectral images provide a visual indicator of any aggregates larger than 4.3 µm. No aggregates were seen for the NISTmAb concentrations at the set temperatures used in this study.

(2) IR spectra are simply 2-point baseline corrected with no data manipulation.

(3) The difference spectra allow us to focus on the changes that are occurring, and also removes the contribution of bulk water in the IR spectra. The spectrum at the initial set temperature is subtracted from all subsequent spectra.

A series of correlation algorithms are then applied to interrogate the data and generate the 2-dimensional plots

(4) Asynchronous 2D-CDS plot

(5) Synchronous 2D-COS plot

(6) Asynchronous 2D-COS plot

2D-COS was introduced during the late 1980's by Noda[4,5], and proven for the analysis of protein applications by others[3]. The algorithm allows for the study of changes in the

secondary structure of proteins and also side chain interactions as a function of external factors. Using this technique, a typical IR spectrum is used as the basis for peak assignments. The use of correlation plots provides enhanced resolution of the peak intensity changes within the spectral region of interest (Figure 1, steps 4-6). If the protein sequence is provided, the location of the changes within the protein are also determined and deamidation can be assigned to specific amino acid(s) (discussed below).

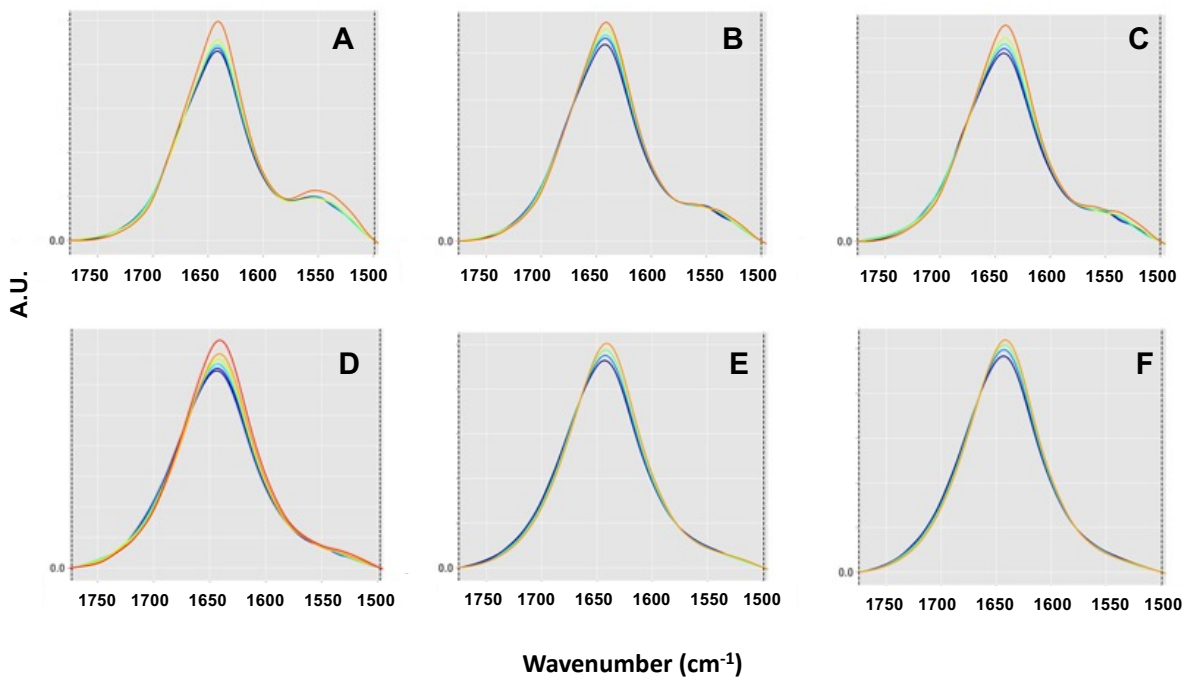

Figure 2: QCLM overlayed spectra of NISTmAb in 25 mM L-histidine at pH 6.0. Concentration of NIST mAb in each overlay are A: 100.0, B: 70.0, C: 40.0, D: 10.0, E: 5.0 and F: 2.5 µg/µL. Linear baseline correction points are shown by vertical dashed lines at 1775 and 1500 cm^{-1}. Intensity differences observed for each sample correspond to the spectrum obtained for each set temperature at 8 °C intervals.

Determining the Extent of Deamidation

Deamidation is associated with thermal stress, low pH or high pH, or a combination of thermal and pH stress. It is a non-enzymatic process so it can identify a specific degradation pathway for a protein therapeutic. The two-step chemical reactions for both asparagine and glutamine deamidation are shown in Figure 3. The deamidation of asparagine or glutamine residues increases the molecular weight of the protein by ~1Da and adds a negative charge to the protein. In the case of asparagine, if the isoaspartate product is formed, an additional carbon atom is introduced to the protein backbone, as shown in Figure 3A.

The vibrational modes of the side chains within the protein change with deamidation and are monitored using the ProteinMentor platform. The changes in intensity of the amides, carbonyls, aspartate and glutamate modes are summarized in Figure 3. In total, 8 peaks plus the backbone vibrational modes are monitored in real-time. The unique design of the ProteinMentor platform and slide cell array allow for the calculation of the extent of deamidation using first principles and the known mechanisms for asparagine and glutamine deamidation. The extent of deamidation for asparagine and glutamine within each secondary structure and for the overall sample is presented in Table 1. For the NISTmAb concentration series, deamidation was most apparent for glutamine within the β-turns of the 100 μg/μL sample. Figure 4 displays the overall deamidation extent as a bar graph for asparagine and glutamine for each point in the dilution series.

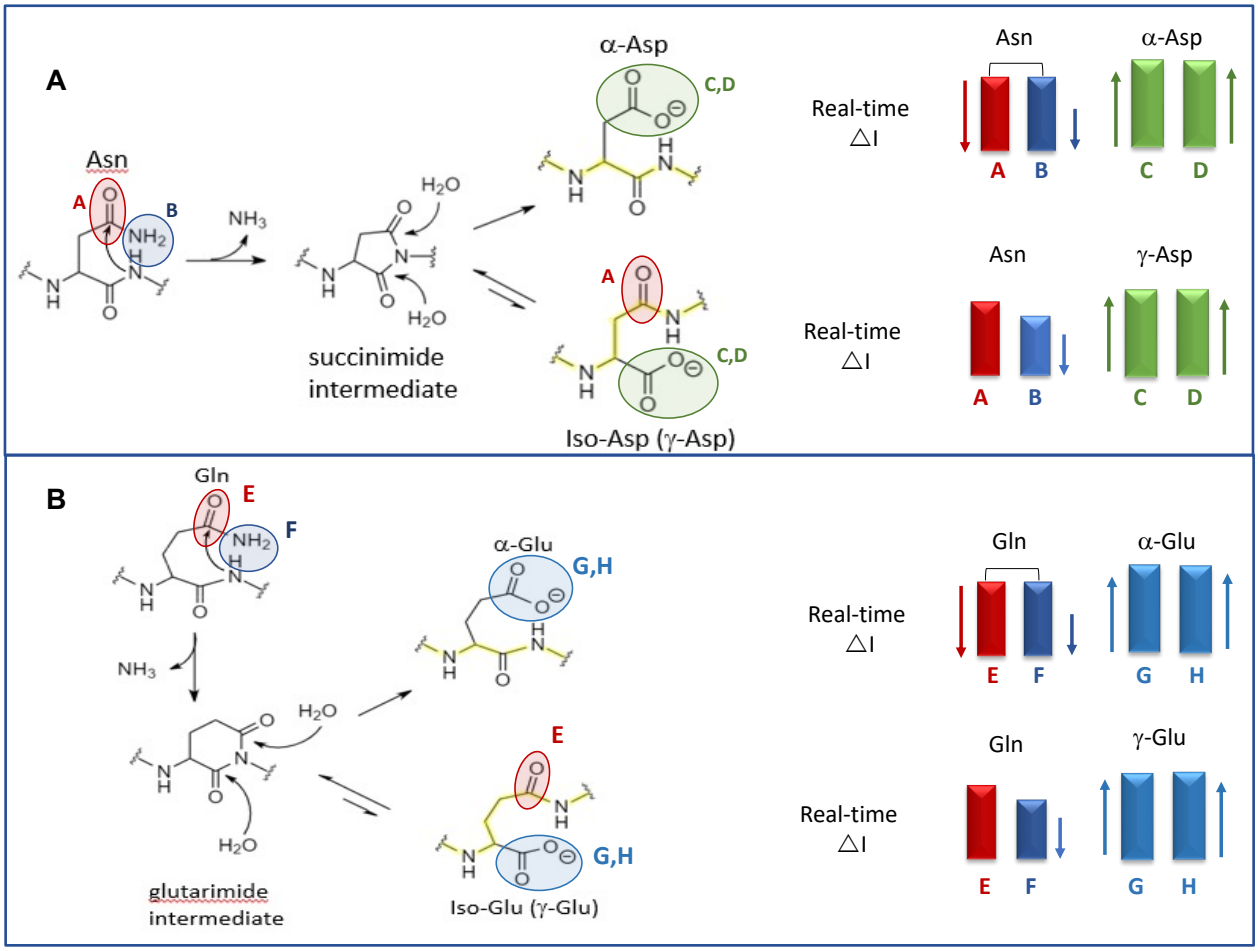

Figure 3: Schematic representing asparagine (A) and glutamine (B) deamidation and vibrational modes (for key functional groups) that are monitored to determine the extent of deamidation. Bar graphs to the right of each scheme correspond to intensity changes for the vibrational modes that are monitored in real-time during the process. The arrows define the direction and the proportionate change in intensity is determined. The change in proportion of the carbonyl and amide vibrational modes (A/B for asparagine and E/F for glutamine) designates if the product is the isoform.

The peak assignments used for asparagine (N) deamidation are represented by the following colors: Red υ(C=O) at 1678 cm^{-1}, Blue $\delta(NH_2)$ at 1612 cm^{-1}, Green: υ(COO-) at 1576 cm^{-1} or 1567 cm^{-1}.

For glutamine (Q) deamidation the colors represent the following modes: Red υ(C=O) at 1670 cm^{-1}, Dark blue $\delta(NH_2)$ at 1581 cm^{-1}, Light blue: υ(COO-) at 1554 cm^{-1} or 1545 cm^{-1}.

Concentration (μg/μL)	Residue	β turn (1696 cm^{-1})		β turn (1681 cm^{-1})		Hinge loop (1663 cm^{-1})		α-helix (1653 cm^{-1})		β sheet (1636 cm^{-1})		Overall Extent of Deamidation	
100	N	0.33	±0.02	0.09	±0.00	0.00	±0.00	0.00	±0.00	0.00	±0.00	0.42	±0.02
	Q	1.35	±0.10	2.01	±0.24	0.00	±0.00	0.00	±0.00	0.00	±0.00	3.36	±0.26
70	N	0.54	±0.17	0.14	±0.01	0.00	±0.00	0.00	±0.00	0.00	±0.00	0.68	±0.17
	Q	0.82	±0.17	0.26	±0.05	0.00	±0.00	0.00	±0.00	0.00	±0.00	1.08	±0.18
40	N	0.26	±0.02	0.12	±0.00	0.00	±0.00	0.00	±0.00	0.00	±0.00	0.38	±0.02
	Q	0.78	±0.08	0.54	±0.04	0.00	±0.00	0.00	±0.00	0.00	±0.00	1.32	±0.09
10	N	0.10	±0.00	0.03	±0.00	0.08	±0.01	0.12	±0.01	0.10	±0.01	0.43	±0.02
	Q	0.10	±0.02	0.02	±0.01	0.00	±0.00	0.00	±0.00	0.00	±0.00	0.12	±0.02
5	N	0.16	±0.02	0.11	±0.01	0.00	±0.00	0.00	±0.00	0.00	±0.00	0.27	±0.02
	Q	0.84	±0.08	0.60	±0.05	0.00	±0.00	0.00	±0.00	0.00	±0.00	1.44	±0.09
2.5	N	0.04	±0.01	0.03	±0.00	0.01	±0.00	0.02	±0.00	0.06	±0.01	0.16	±0.01
	Q	0.17	±0.01	0.04	±0.01	0.42	±0.02	0.00	±0.00	0.00	±0.00	0.63	±0.02

Table 1: The extent of deamidation associated within each secondary structure type of the NISTmAb concentration series and the overall (summed) extent of deamidation. Each value represents the number (or fraction) of deamidation sites within each secondary structure and the overall protein. The error propagation associated with each measurement is included.

For example, glutamine deamidation was apparent within the β-turns of the 100 μg/μL sample (highlighted in the dotted line box of the β-turn columns). A value of 2 indicates that over the course of the thermal perturbation, two glutamine sites underwent deamidation. This likely corresponds to a single site within both chains of the NIST mAb dimer (identification of the site of deamidation is explained below).

The workflow provides the capability of analysis of the intact, full-length protein in solution, without the need for buffer exchange or sample digestion. The extent of both asparagine and glutamine deamidation is therefore evaluated across all sample concentrations for each secondary structure and the overall intact protein in its native state (including the quaternary structure).

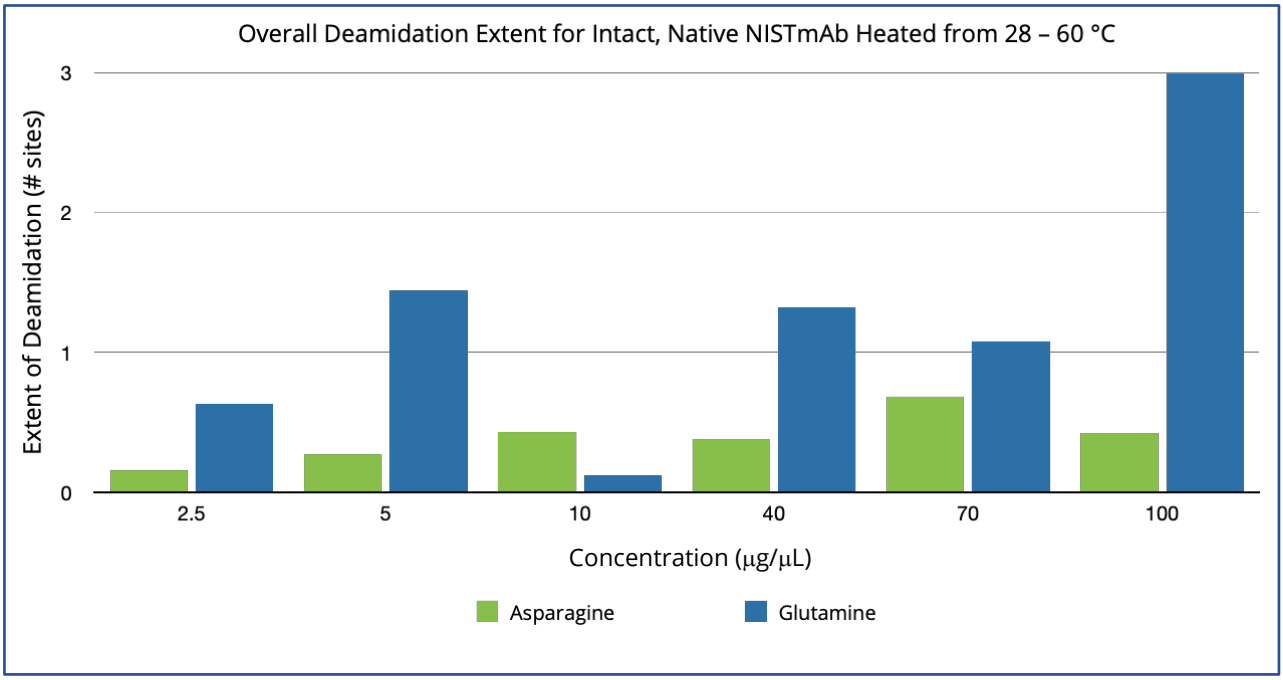

Figure 4: Bar graph of the overall extent of asparagine (green) and glutamine (blue) deamidation for the full-length, native NISTmAb as a function of concentration over the thermal ramp. The greatest risk of deamidation was apparent for glutamine in the 100 μg/μL sample of NISTmAb.

Determining the Site of Deamidation

When the sequence of the protein is provided, identification of the site of deamidation can also be determined, based on perturbation of neighboring residues due to the deamidation process. There are multiple potential sites for deamidation. If there is a deamidation event occurring at one specific site, perturbations due to that deamidation process can be seen in neighboring residues, and within the secondary structure.

Changes in the peaks associated neighboring residues of potential deamidation sites are monitored. Identifying other residues that are perturbed at the same time as the deamidation event enables location of the deamidation site. There are typically multiple residues that would be perturbed around a deamidation event and those are used as pre-requisites to confirm the site of deamidation.

Figure 5 shows a schematic of the process used to determine the site of deamidation. It is the asynchronous plot from 2D-COS, that is used for analysis of the site of deamidation as this plot results in enhanced resolution allowing for in-depth analysis. The asynchronous plot describes the changes in intensity that are out of phase from one other. The plot is symmetrical but inverted in direction along the center diagonal. The upper triangle is used to determine the molecular order of events and thereby the site of deamidation.

The data is used assess the deamidation for each secondary structure, whether it be the beta turns, or the alpha helices, for example, by looking at the vertical position of the peak (the υ1 axis). In Figure 5A, υ1 for the β-turns is highlighted at 1696 cm^{-1}. Correlated peaks on the υ2 axis for asparagine (1678 and 1612 cm^{-1}) and aspartate (1572 and 1567 cm^{-1}) vibrational modes are circled in white and red, respectively (Figure 5A). For each correlated wavenumber pair (υ1, υ2) the intensity of the change is given by the color in the asynchronous plot and has also been represented by a bar graph in Figure 5B for the asparagine/aspartate modes within the β-turns.

The molecular order of events is then determined using a set of rules established by Noda[4,5]. The 2-D COS intensity sign determines the order. For negative peaks, wavenumber υ1 (the x axis) changes after the wavenumber υ2 (the y axis). For the asparagine correlated with the β-turn circled in Figure 5A (υ1: 1696 cm^{-1}, υ2: 1612 cm^{-1}), the beta turn change happens after the asparagine deamidation because the peak is negative.

In contrast, for the aspartate intensity changes (e.g. υ1: 1696 cm^{-1}, υ2: 1572 cm^{-1}), the beta turn changes happen before the second step of the deamidation, which is the hydrolysis to form aspartate.

The cumulative level of information established using logic with Noda's rules allows for the determination of the sequential order of molecular events. Combined with knowledge of the neighboring residues of potential deamidation sites, the site(s) of deamidation can be determined. Perturbations to residues that neighbor a deamidation event are significant, owing to the introduction of the negative charge. A full description of the specific changes for NISTmAb at each concentration is described in reference 3. The correlational analysis allowed for the determination of the specific sites of deamidation within NISTmAb.

Figure 6 shows a summary of the sites of deamidation identified for the NISTmAb 100 μg/μL sample in the study. The highest risk of deamidation was apparent for glutamine within the β-turns at 100 μg/μL as seen in Table 1 and Figure 4. These site(s) are on the heavy chain, located within the constant Fc region at Q421 and/or Q422 (underlined in blue, Figure 6). A smaller degree of deamidation was apparent for N437 of the 100 μg/μL sample (underlined in green, Figure 6). For the other concentrations of NISTmAb, deamidation risk was also apparent for glutamines within the light chain, Q36 and Q154. Risk of asparagine deamidation was identified at sites within the heavy chain at N437 and N318 and within the light chain at N157.

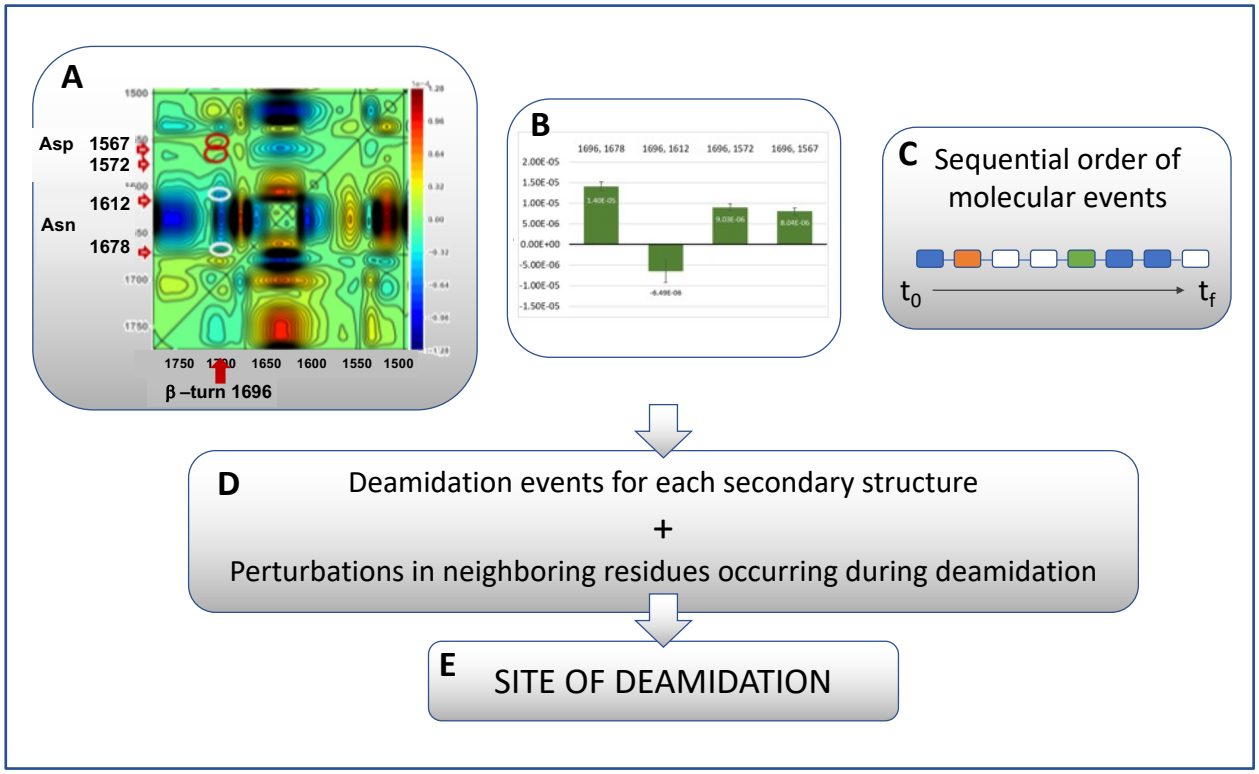

Figure 5: Schematic for the process to identify sites of deamidation using ProteinMentor and 2-D COS.

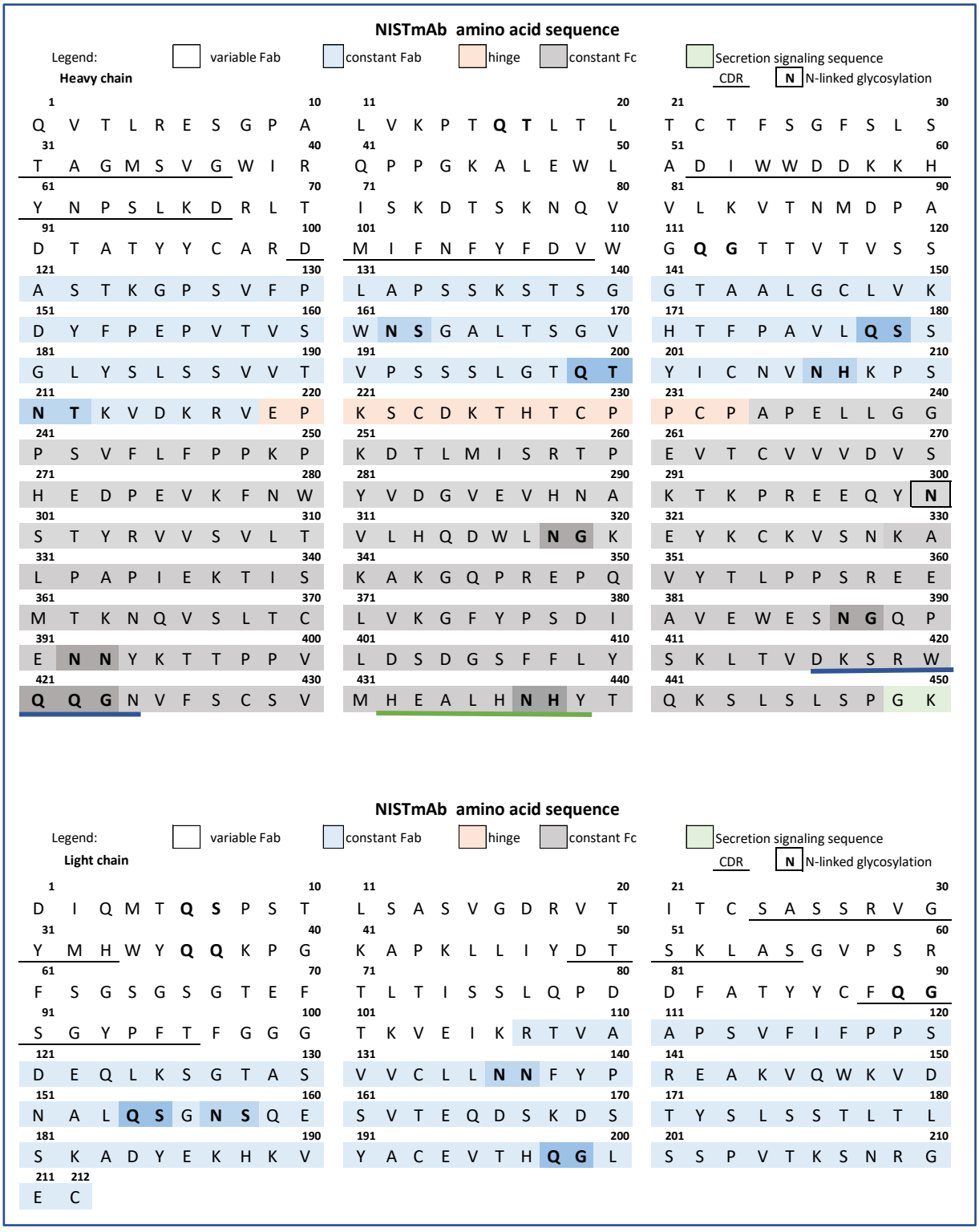

Figure 6: Amino acid sequence of NISTmAb showing a summary of potential deamidation based on the amino acid sequence evaluation[8,9] shown in bold type. The actual sites of deamidation apparent for the thermal perturbation of the 100 µg/µL sample of NISTmAb are shown by the

blue (Q421/Q422) and green (N437) underlined sections. The region underlined include the sites of deamidation along with the neighboring residues that were monitored to determine the site of deamidation.

Comparison with Molecular Model and Published Results

The spatial location of the deamidation sites identified in this study were used for the generation of structural models from the available high-resolution structures for NISTmAb (PDB ID 5KD8 for the Fab region and PDB ID: 5VGP for the Fc region)[6,7]. The model generated for the Fc region is shown in Figure 7, and highlights the spatial location of the deamidation sites and also their solvent accessibility. Overall, there was no risk of deamidation observed for the CDRs, which is a critical consideration for any impact on target binding.

Many reports have been published on asparagine deamidation, however, glutamine deamidation has been less widely reported. For NISTmAb, sites of both forced and spontaneous deamidation on asparagine and glutamine residues have been reported. The deamidation sites that were identified in the heavy chain (N318, N437 and Q421/422) and the light chain (N157, Q36 and Q154) in this study are in agreement with published LC-MS studies by multiple groups, different instruments and different sample preparation protocols[6,11-16].

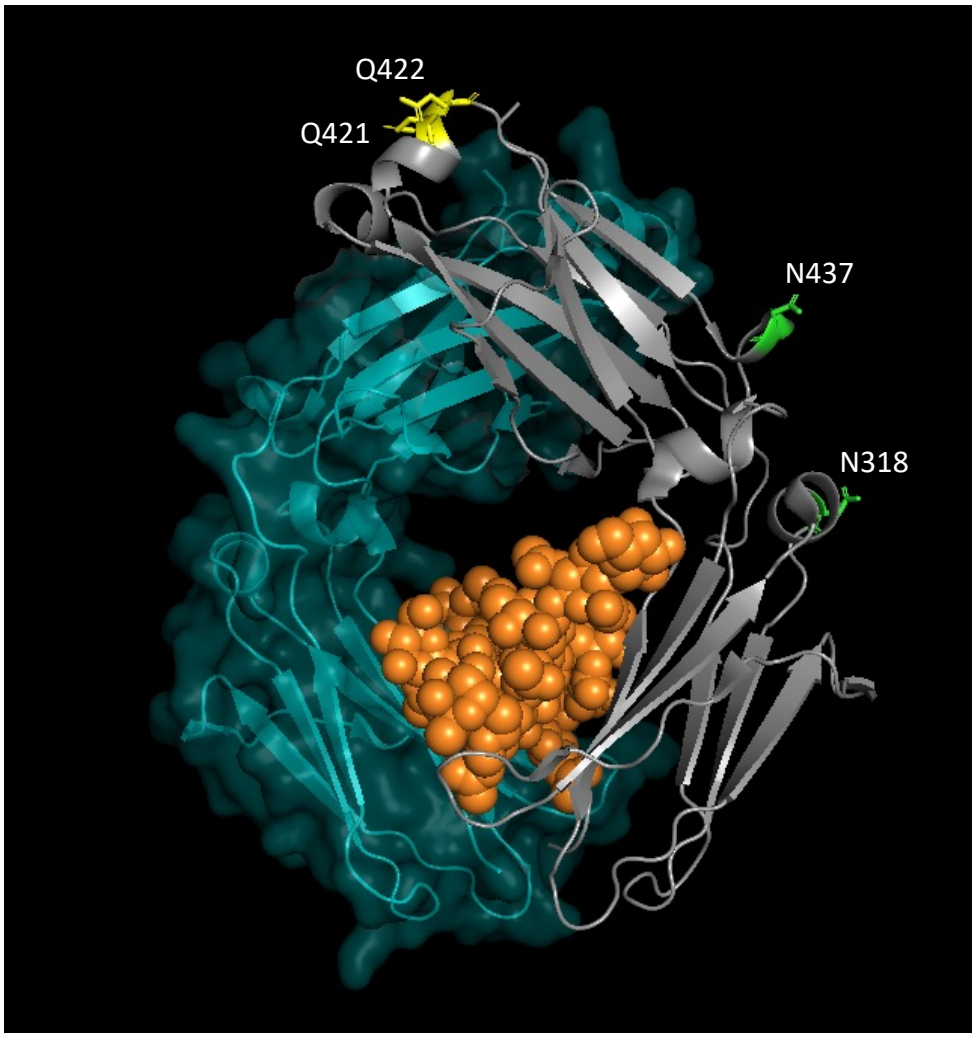

Figure 7: NISTmAb Fc high resolution structure representation (PDB ID: 5VGP). The Fc region is comprised exclusively of the heavy chain (HC) component. The model was generated as a combined (dark grey) ribbon and (dark cyan) transparent surface with ribbon representation to highlight the symmetry of the homodimer. Also, represented as orange spheres are the glycosylation components of the NISTmAb. Only one of the dimer components (dark grey) chain A, shows the deamidation site labels. The deamidation sites for the Fc region are: (green sticks) asparagine (N) and (yellow sticks) glutamine (Q). All deamidation sites within the Fc HC are exposed to the aqueous environment. In addition, these asparagine and glutamine deamidation sites do not impact the CDR regions, yet induce self-association of the NISTmAb. The model representation was generated using the PyMOL Molecular Graphics System, Version 2.3, Schrödinger, LLC.

Conclusions

The ProteinMentor platform allows for the real-time acquisition of hyperspectral images for an array of therapeutic proteins in solution under controlled thermal perturbation.

The experiment described here, (from 28-60 °C) took less than 2 hours and used only 1 µL sample per well.

The approach does not require sample digestion or separation techniques but instead uses real-time monitoring of signature peaks that are indicative of the deamidation process.

2D-COS analysis of the difference spectra enabled correlation of the signature peaks with their secondary structure and identification of neighboring residues that were impacted by the deamidation process.

The results of correlational analysis were then used to determine the sequential order of molecular events and identification of the sites of deamidation.

The direct monitoring of both asparagine and glutamine deamidation of the full-length protein in its formulation without sample preparation is a major advantage for biopharmaceutical scientists and engineers.

Protein Dynamic Solutions
Wakefield, Massachusetts
USA
www.pdsbio.com
info@pdsbio.com

References:

1. Antibody Society, Inc. https://www.antibodysociety.org/

2. Kaplon, H. and Reichart, J.M., "Antibodies to watch in 2021" *MABS,* 13:e1860476 (34 pages) 2021. https://DOI.org/10.1080/19420862.2020.1860476.

3. Pastrana, B., Meuse, C.W., "Two-Dimensional Correlation and Two-Dimensional Co-Distribution Spectroscopies of Proteins" *Encyl. Anal. Chem.*, 29 September, 2022, "Two-dimensional correlation spectroscopy of protein dynamics" Ed Meyers, R., https://doi.org/10.1002/9780470027318.a9792

4. Noda, I. Dowrey, A.E. Marcott, C. Story, G.M. Ozaki, Y. "Generalized two-dimensional correlation spectroscopy" *Appl. Spectrosc.*, 2000, 54, 236A-248A. https://doi.org/10.1366/0003702001950454

5. Noda, I. "Techniques useful in two-dimensional correlation and co-distribution spectroscopy (2DCOS and 2DCDS) analyses" *J. Mol. Struct.*, 2016, 1124, 29e41. https://doi.org/10.1016/j.molstruc.2016.01.089

6. D.T. Gallagher, Karageorgos, I. Hudgens, J.W. Galvin, C.V. 'Data on crystal organization in the structure of the Fab fragment from the NIST reference antibody RM8671,' Data Brief., 16, 29 (2018). https://doi.org/10.1016/J.DIB.2017.11.013

7. D.T. Gallagher, Connor V.G. and Karageorgos, I. 'Structure of the Fc fragment of the NIST reference antibody RM8671,' Acta Crystallogr. F Struct. Biol. Commun., 74, 524-529 (2018). https://doi.org/10.1107/S2053230X18009834

8. Robinson, N.E., Robinson, Z.W., Robinson, B.R., Robinson, A.L., Robinson, J.A., Robinson, M.L., Robinson, A.B., 'Structure-dependent nonenzymatic deamidation of glutaminyl and asparaginyl pentapeptides', *J. Pept. Res.*, 2004, 63, 426−436. https://doi.org/10.1111/j.1399-3011.2004.00151.x

9. Wright, H.T., 'Nonenzymatic deamidation of asparaginyl and glutaminyl residues in proteins', *Crit. Rev. Biochem. Mol. Biol*., 1991, 26, 1–52. https://doi.org/10.3109/10409239109081719

10. Millán-Martín, S. Jakes, C. Dorival-García, N. McGillicuddy, N. Carillo, S. Farrell, A. Bones, J. (2018) 'Comparison of alternative approaches to trypsin protein digestion for reproducible and efficient peptide mapping analysis of monoclonal antibodies', 2018, AN21782-EN 0718S. https://www.separatedbyexperience.com/documents/an-21782-lc-ms-peptide-map-digest-comparison-an21782-en.pdf

11. Formolo, T., Ly, M., Levy, M., Kilpatrick, L., Lute, S., Phinney, K., Marzilli, L., Brorson, K., Boyne, M., Davis, D., Schiel, J., Chapter 1 Determination of the NISTmAb Primary Structure" *State-of-the-Art and Emerging Technologies for Therapeutic Monoclonal Antibody Characterization"* , Volume 2. Biopharmaceutical Characterization: The NISTmAb Case Study ACS Symposium Series; American Chemical Society: Washington, DC, 2015. https://doi.org/10.1021/bk-2015-1201.ch001

12. Nowak, C., Tiwari, A., Liu, H. –c., 'Asparagine Deamidation in a Complementarity Determining Region of a Recombinant Monoclonal Antibody in Complex with Antigen', *Anal. Chem*., 2018, 90, 6998−7003. https://doi.org/10.1021/acs.analchem.8b01322

13. Mouchahoir, T., Schiel, J. E., 'Development of an LC-MS/MS peptide mapping protocol for the NISTmAb', *Anal. Bioanal. Chem*., 2018, 410, 2111-2126. https://doi.org/10.1007/s00216-018-0848-6

14. Huang, L., Lu, J., Wroblewski, V. J., Beals, J. M., Riggin, R. M., 'In vivo deamidation characterization of monoclonal antibody by LC/MS/MS', *Anal. Chem.,* 2005, 77, 1432–1439.https://doi.org/10.1021/ac0494174

15. Beck, A., Liu, H. –c. 'Macro- and Micro-Heterogeneity of Natural and Recombinant IgG Antibodies', *Antibodies*, 2019, 8, 18-24. https://doi.org/10.3390/antib8010018

16. Faist, J. Capasso, F., Sivco, D.L., Sirtori, C., Hutchinson, A.L., Cho, A.Y., 'Quantum cascade laser,' *Science*, 264, 553-556, 1994. https://DOI: 10.1126/science.264.5158.553.